THE JOURNAL OF BIOLOGICAL CHEMISTRY VOL. 287, NO. 44, pp. 36883–36895, October 26, 2012

N-Myristoylation and Ca^{2+} Binding of Calcineurin B Homologous Protein CHP3 Are Required to Enhance Na^+/H^+ Exchanger NHE1 Half-life and Activity at the Plasma Membrane*[S]

Received for publication, June 22, 2012, and in revised form, August 30, 2012 Published, JBC Papers in Press, September 14, 2012, DOI 10.1074/jbc.M112.394700

Hans C. Zaun, Alvin Shrier, and John Orlowski[1]

From the Department of Physiology, McGill University, Montréal, Québec H3G 1Y6, Canada

Background: CHP3 is an *N*-myristoylated Ca^{2+}-binding protein that up-regulates the cell surface expression and stability of the Na^+/H^+ exchanger NHE1 isoform.
Results: *N*-Myristoylation or the Ca^{2+}-binding site of CHP3 regulates the half-life and activity of NHE1 at the cell surface.
Conclusion: CHP3 possesses a Ca^{2+}-myristoyl switch mechanism to promote optimal NHE1 activity at the cell surface.
Significance: These findings provide fundamental insight into the molecular mechanisms that regulate NHE1.

Calcineurin B homologous proteins (CHP) are *N*-myristoylated, EF-hand Ca^{2+}-binding proteins that regulate multiple cellular processes, including intracellular pH homeostasis. Previous work has shown that the heart-enriched isoform, CHP3, regulates the plasmalemmal Na^+/H^+ exchanger NHE1 isoform by enhancing its rate of oligosaccharide maturation and exocytosis as well as its half-life and transport activity at the cell surface (Zaun, H. C., Shrier, A., and Orlowski, J. (2008) *J. Biol. Chem.* 283, 12456–12467). However, the molecular basis for this effect is not well understood. In this report, we investigated whether the *N*-myristoylation and Ca^{2+}-binding domains of CHP3 are important elements for regulating NHE1. Mutation of residues essential for either *N*-myristoylation (G2A) or calcium binding (D123A) did not prevent the interaction of CHP3 with NHE1, although the D123A mutant no longer showed elevated binding to NHE1 in the presence of Ca^{2+} when assessed using *in vitro* binding assays. Disruption of either site also did not impair the ability of CHP3 to stimulate the biosynthetic processing and trafficking of NHE1 to the plasma membrane nor did it affect the H^+ sensitivity of the exchanger. However, they did significantly reduce the cell surface half-life and near maximal transport velocity of NHE1 to a similar extent. Simultaneous mutation of both sites (G2A/D123A) gave results identical to the individual substitutions. This finding suggests that both domains in CHP3 are interdependent and may function cooperatively as a Ca^{2+}-myristoyl switch mechanism to selectively stabilize the NHE1·CHP3 complex at the cell surface in a conformation that promotes optimal transport activity.

Regulation of intracellular pH (pH_i) is a fundamental physiological process of all living cells. In mammals, precise control of pH_i involves the coordinated activities of several distinct solute carriers that conduct the transmembrane fluxes of H^+ or HCO_3^-, usually directly coupled to the movement of another ion (1). Of these, one of the major mechanisms for protecting cells from excess intracellular acidification involves the coupled countertransport of alkali cations such as Na^+, but in some cases also K^+, for H^+ across the cell surface and are simply referred to as Na^+/H^+ exchangers or antiporters (NHE^2/NHX/NHA).

The NHE1 isoform has been studied extensively because it is present in most cells and makes vital contributions to not only cytoplasmic pH homeostasis but also an array of other physiological processes, such as cell volume regulation (2), shape (3), adhesion and spreading (4), migration (5), proliferation (2, 6), differentiation (7, 8), and apoptosis (9, 10). The central involvement of NHE1 in such diverse physiological phenomena has prompted searches for unique as well as common regulatory factors that might underlie these relationships. Not surprisingly, numerous hormones, growth factors, and second messengers such as Ca^{2+} have been found to regulate NHE1 activity by either phosphorylation-dependent or -independent mechanisms that, in several cases, involve the subsequent binding of various effector molecules to the cytoplasmic C terminus of the transporter (11–13). One such class of interacting proteins is a family of *N*-myristoylated, EF-hand Ca^{2+}-binding proteins called the calcineurin B homologous proteins (CHPs) (14).

The CHP proteins are of particular interest because they are critical for optimal basal as well as stimulus-mediated regulation of the plasmalemmal NHEs. They compose a family of three isoforms (CHP1–CHP3) that share homology with the calcineurin B subunit of the phosphatase, calcineurin, and indeed are capable of regulating the phosphatase activity of the calcineurin A catalytic subunit (15, 16). CHP1 (also known as p22) is widely expressed and sets the resting pH_i sensitivity of NHE1 in the physiological neutral range, but it also confers

* This work was supported by Grants MOP 11221 (to J. O.) and MOP 86589 (to A. S.) from the Canadian Institutes for Health Research.
[S] This article contains supplemental Figs. S1–S3 and additional references.
[1] To whom correspondence should be addressed: Dept. of Physiology, McGill University, McIntyre Medical Science Bldg., 3655 Promenade Sir-William-Osler, Montreal, Quebec H3G 1Y6, Canada. Tel.: 514-398-8335; Fax: 514-398-7452; E-mail: john.orlowski@mcgill.ca.

[2] The abbreviations used are: NHE, Na^+/H^+ exchanger; CHP, calcineurin B homologous protein; AP-1, a chemically mutagenized CHO cell line that is devoid of plasma membrane Na^+/H^+ exchange activity.

responsiveness to various signaling molecules (17, 18). By contrast, CHP2 expression is detected mainly in normal intestinal epithelia (19), but it is induced in several malignant cell types where it constitutively enhances the pH_i sensitivity of NHE1 in the absence of peripheral stimulatory signals, resulting in a more alkaline cytoplasm that promotes their survival (20–22). The third isoform of the CHP family, CHP3 or tescalcin, was originally discovered as an autosomal gene whose mRNA transcript was detected in mouse developing testis (23). However, in adult animals, its expression is restricted mainly to heart, brain, stomach, and hematopoietic cells (16, 24). Functionally, CHP3 is distinguished by its ability to positively enhance multiple biochemical properties of NHE1. These include elevating its rate of post-translational maturation along the exocytic pathway, its half-life at the plasma membrane, and its maximal transport velocity without affecting its intracellular H^+ affinity (25). A more recent study indicated that increased stabilization of the NHE1 protein may also be conferred by the CHP1 isoform (26).

How the CHP proteins are able to differentially modulate various facets of NHE1 function is poorly understood. Previous studies have shown that all three CHP proteins contain an *N*-myristoylated consensus site and at least one functional EF-hand Ca^{2+}-binding domain (16, 17). *N*-Myristoylation is known to promote the reversible tethering of proteins to the inner leaflet of membrane bilayers, thereby providing an effective means of controlling the membrane targeting and function of certain soluble proteins (27, 28). By comparison, EF-hand Ca^{2+}-binding proteins are known to undergo Ca^{2+}-dependent conformational changes that modulate their function or influence the activity of their effectors (29). Interestingly, some proteins contain both elements that function cooperatively as a Ca^{2+}-myristoyl switch to control specific calcium-sensitive membrane processes (30). However, in the case of the NHE1·CHP1 complex, the Ca^{2+}-myristoyl switch mechanism does not appear operational as it binds Ca^{2+} constitutively to two of its four predicted EF-hand motifs (EF3 and EF4) due to its high nanomolar affinity for Ca^{2+} (apparent $K_d \sim 2$ nM) under resting physiological conditions (17, 18). Mutation of its myristoylation site did not affect the membrane trafficking or activity of NHE1, whereas disruption of either Ca^{2+}-binding domain significantly reduced the H^+ affinity and activity of the exchanger as well as its responsiveness to various stimuli (17). Hence, it was proposed that the Ca^{2+}-binding domains in CHP1 might serve a more structural rather than Ca^{2+}-sensing/regulatory role. By comparison, CHP3 contains only a single functioning EF-hand Ca^{2+}-binding domain (EF3) that binds Ca^{2+} with lower micromolar affinity and therefore may behave differently than CHP1 (16).

In this study, we investigated this possibility and found that *N*-myristoylation and Ca^{2+} binding of CHP3 are not required for the interaction between NHE1 and CHP3 nor are they necessary for CHP3 to enhance the biosynthetic maturation of NHE1. However, Ca^{2+} enhances CHP3 binding to NHE1, and loss of either *N*-myristoylation or Ca^{2+} binding similarly decreased the stability and transport activity of NHE1 at the cell surface. Simultaneous disruption of both sites gave results comparable with the individual mutations. This finding suggests that both domains in CHP3 are structurally linked and may operate as a Ca^{2+}-myristoyl switch mechanism to selectively stabilize the NHE1·CHP3 complex at the cell surface in an arrangement that enables optimal exchange activity.

EXPERIMENTAL PROCEDURES

Materials—Monoclonal antibodies to a decapeptide derived from influenza virus hemagglutinin (HA) were purchased from Covance Inc. (Berkeley, CA) and to the peptide of the c-*myc* proto-oncogene (*myc*) from Millipore (Temecula, CA). Polyclonal antibodies to the HA-epitope and Myc epitope were purchased from Abcam Inc. (Cambridge, MA) and Upstate Biotechnology, Inc. (Lake Placid, NY), respectively, and antibodies specific to glyceraldehyde-3-phosphate dehydrogenase (GAPDH) were purchased from Abcam. All Alexa Fluor®-conjugated goat anti-mouse or anti-rabbit IgG antibodies were purchased from Molecular Probes (Eugene, OR).

Vent polymerase, DNA ligase, restriction endonucleases, as well as protein and DNA markers were purchased from New England Biolabs (Ipswich, MA). α-Minimum essential medium, fetal bovine serum (FBS), penicillin/streptomycin, geneticin (G418), trypsin-EDTA, and Lipofectamine-2000™ transfection reagent were all purchased from Invitrogen. Carrier-free ^{22}NaCl (range of specific activity, 900–950 mCi/mg; concentration, ~10 mCi/ml) was obtained from PerkinElmer Life Sciences. Amiloride hydrochloride, nigericin, and ouabain were all purchased from Sigma, and complete protease inhibitor mixture tablets were obtained from Roche Diagnostics. All other chemicals and reagents were purchased from BioShop Canada (Burlington, Ontario, Canada), Sigma, or Fisher and were of highest grade available.

cDNA Construction and Mutagenesis—A mammalian expression vector under the control of the enhancer/promoter region from the immediate early gene of human cytomegalovirus (pCMV) and expressing either the cDNA of NHE1 containing a C-terminal hemagglutinin (HA) epitope tag ($NHE1_{HA}$) or CHP3/tescalcin cDNA constructed to contain a Myc epitope at its C terminus ($CHP3_{myc}$) were constructed as described previously (25).

Mutations that disrupt the *N*-myristoylation (G2A) and EF-hand Ca^{2+}-binding sites (D123A) of $CHP3_{myc}$ as identified by Gutierrez-Ford *et al.* (16) were accomplished by PCR mutagenesis. All constructs were sequenced to confirm the presence of the desired mutations and to ensure that other random mutations were not introduced.

Cell Culture and Transfection—A cell line devoid of endogenous Na^+/H^+ exchanger activity derived from Chinese hamster ovary fibroblasts (CHO), termed AP-1 (31), was maintained in α-minimum essential medium supplemented with 10% fetal bovine serum, penicillin/streptomycin (100 units/ml/100 μg/ml), and 25 mM sodium bicarbonate. Cells were incubated in a humidified atmosphere of 95% air, 5% CO_2 at 37 °C. For AP-1 cells expressing either $NHE1_{HA}$ or coexpressing $NHE1_{HA}$ along with either wild-type or mutated $CHP3_{myc}$, a total of 2 μg of DNA was transfected in a 6-well plate using Lipofectamine™-2000 reagent according to the manufacturer's recommended procedure. Twenty four hours post-transfection, the cells were split into 10-cm dishes at a dilution of 1:10 and 1:50 and then selected for cells that stably express

$NHE1_{HA}$ by testing for their ability to survive repeated challenges of intracellular acid loading over a 2-week period, as described previously (32). Cells stably expressing $CHP3_{myc}$ were selected in α-minimum essential medium culture medium supplemented with the aminoglycoside antibiotic geneticin (G418) (600 μl/ml) over a 2–4-week period.

Coimmunoprecipitation and Western Blotting—Coimmunoprecipitations of wild-type $NHE1_{HA}$ and wild-type or mutant forms of $CHP3_{myc}$ (G2A, D123A, and G2A/D123A) were performed in 10-cm dishes by transfecting AP-1 cells stably expressing $NHE1_{HA}$ with 10 μg of the desired $CHP3_{myc}$ constructs using Lipofectamine™-2000 according to the manufacturer's recommended procedure. Twenty four hours post-transfection, cell lysates were obtained by washing cells in ice-cold PBS and adding 1 ml of radioimmunoprecipitation (RIPA) buffer (150 mM NaCl, 50 mM Tris, 1 mM EDTA, 2.5% deoxycholate, 0.5% Nonidet P-40, and protease inhibitors). For Ca^{2+} dependence of $NHE1_{HA}$/$CHP3_{myc}$ coimmunoprecipitation, RIPA buffer was either supplemented with 1 mM Mg^{2+} and 2 mM EDTA or 0.1 mM Ca^{2+} without EDTA. Cell were scraped from the dish and incubated for 20 min at 4 °C, followed by centrifugation for 20 min at 4 °C to pellet cellular debris. Supernatants were then pre-cleared with 100 μl of a 50% protein G-Sepharose (GE Healthcare) slurry for 2 h at 4 °C. After brief centrifugation to remove the protein G-Sepharose and retaining a small fraction for Western blotting, the remaining supernatants were incubated with 5 μl of primary rabbit polyclonal antibody against either the HA or Myc epitope and incubated overnight at 4 °C with gentle rocking. Protein G-Sepharose (100 μl) was then added and incubated for 6 h at 4 °C with gentle rocking, followed by multiple washes with RIPA buffer to remove nonbound proteins. Protein conjugates were then eluted by SDS sample buffer (2% SDS, 50 mM Tris·HCl, pH 6.8, 100 mM dithiothreitol) by incubating samples for 30 min at room temperature without boiling to prevent aggregation of NHE1 proteins. Samples were then subjected to SDS-PAGE, transferred to polyvinylidene fluoride (PVDF) membranes (Millipore, Bedford, MA), and subjected to Western blotting. Membranes were blocked with 5% nonfat powdered milk and incubated with a primary mouse monoclonal antibody recognizing either the HA epitope (1:10,000 dilution) or the Myc epitope (1:1000 dilution). After several washes with PBS containing 0.1% Tween 20, blots were incubated with a secondary goat anti-mouse antibody conjugated to horseradish peroxidase (HRP) at a dilution of 1:10,000. Immunoreactive bands were then visualized using the Western Lightning™ Plus-ECL Western blotting detection reagents (PerkinElmer Life Sciences).

Immunocytochemistry—AP-1 cells alone or stably expressing $NHE1_{HA}$ were grown to subconfluence on glass coverslips treated with 1.5 μg/ml fibronectin (Sigma) and then transfected with 2 μg of either $CHP3_{myc}$ wild-type or mutant constructs using Lipofectamine™-2000 according to the manufacturer's recommendations. Twenty four hours post-transfection, cells were washed with PBS and fixed in 2% paraformaldehyde/PBS for 30 min. Cells were then permeabilized in PBS containing 0.1% saponin for 30 min followed by repeated washing with 10 mM glycine in PBS, 0.01% saponin buffer. After blocking for 1 h in PBS, 10% goat serum, 0.01% saponin, cells were incubated with a combination of a mouse monoclonal anti-HA antibody (1:1000) and a rabbit polyclonal anti-Myc antibody (1:500) or a rabbit polyclonal anti-HA antibody (1:500) along with a mouse monoclonal anti-Myc antibody (1:250) overnight at 4 °C. All antibodies were diluted in PBS containing 10% goat serum and 0.01% saponin. After several washes with PBS, 0.01% saponin, cells were incubated with secondary goat anti-mouse and anti-rabbit antibodies conjugated to Alexa Fluor™-488 and Alexa Fluor™-569, respectively, at a dilution of 1:2000 in PBS, 10% goat serum, 0.01% saponin for 2 h at room temperature. Coverslips were subsequently washed several times in PBS, 0.01% saponin and mounted onto glass slides with ImmunoFluore™ mounting medium (ICN Biomedicals, Aurora, OH). Transfected cells were analyzed by laser scanning confocal microscopy using a Zeiss LSM 510, and images were analyzed using Zen 2011 (Carl Zeiss Microscopy) and Imaris (Bitplane Inc., CT) software.

The degree of colocalization between $NHE1_{HA}$ and the various $CHP3_{myc}$ constructs was estimated by calculating the Pearson's correlation coefficient (*r*) (value between −1 and +1). This mathematical parameter is a statistical analysis of the relationship or degree of overlap between different fluorescence signals. An *r* value greater than 0.5 indicates a high degree of colocalization; 0.3–0.5 indicates medium correlation; 0 implies no linear correlation, and −1 implies that all data points lie on a line for which one signal decreases as the other increases (33).

Measurement of Na^+/H^+ Exchanger Activity—AP-1 cells expressing $NHE1_{HA}$ alone or in combination with different $CHP3_{myc}$ constructs (wild-type, G2A, D123A, and G2A/D123A) were grown to confluence in 24-well plates. NHE1 activity was assessed using a radioisotope influx assay. Briefly, to measure NHE1 activity at near maximal velocity, cells were acidified using the NH_4Cl technique, and the initial rates of $^{22}Na^+$ influx were measured in the absence and presence of the NHE1 inhibitor amiloride (1 mM), as described previously (25). NHE1 activity was defined as the amiloride-inhibitable fraction of the total radioisotope influx. Protein content was determined using the Bio-Rad *DC* protein assay procedure.

To measure the NHE1 activity as a function of the expression of the different $CHP3_{myc}$ constructs, 10-cm dishes of AP-1 cells stably expressing $NHE1_{HA}$ were grown to subconfluence and transfected with an increasing ratio of $CHP3_{myc}$-containing plasmids relative to empty vector (0–10 μg) using Lipofectamine™-2000. Twenty four hours post-transfection, cells were split into 24-well plates (6-wells per transfection) for NHE1 activity measurements as well as a 6-well plate (1-well per transfection) for parallel Western blotting analyses; the cells were incubated for a further 24 h prior to the analyses. $NHE1_{HA}$ activity was also measured as a function of the intracellular H^+ concentration (pH_i) by clamping pH_i over the range of 5.4 to 7.4 using the K^+/H^+ exchange ionophore nigericin as described previously (34).

Cell Surface Biotinylation and Pulse-Chase Assay—To determine the relative amount of cell surface $NHE1_{HA}$ as a function of the expression of $CHP3_{myc}$ (wild-type, G2A, D123A, G2A/D123A), we used a cell surface biotinylation assay as described

previously (25). Briefly, AP-1 cells were grown to subconfluence on 10-cm dishes and transfected with 8 μg of expression vector containing $NHE1_{HA}$ along with an increasing ratio of the different $CHP3_{myc}$ cDNA constructs (0–2 μg) to empty expression vector using Lipofectamine™-2000. A green fluorescent protein (GFP) expression vector (1 μg) was also transfected as a control for transfection efficiency. Forty eight hours post-transfection, cells were placed on ice, and surface proteins were covalently modified with sulfo-NHS-SS-biotin (Thermo Scientific, Rockford, IL), a water-soluble, membrane-impermeable, thiol-cleavable, and amine-reactive biotinylation reagent. Following the addition of quenching buffer (20 mM glycine in PBS), cell lysates were obtained in RIPA buffer by scraping cells and incubating for 20 min on ice, followed by centrifugation for 20 min to remove cellular debris. A small fraction of supernatant was removed for Western blotting, and the remaining supernatant was incubated with a 50% NeutrAvidin®-agarose slurry (Thermo Scientific) in RIPA buffer overnight at 4 °C. The bound biotinylated protein complexes were isolated by centrifugation and then subjected to SDS-PAGE and immunoblot analyses.

The cell surface stability of $NHE1_{HA}$ in relation to the expression of $CHP3_{myc}$ wild-type or mutants was determined through a pulse-chase of biotinylated NHE_{HA} as described previously (25). Briefly, 6-well plates containing AP-1 cells expressing either NHE_{HA} alone or coexpressing NHE_{HA} along with $CHP3_{myc}$ wild-type or mutants forms (G2A, D123A, G2A/D123A) were grown to ~90% confluence, and cell surface proteins were biotinylated and quenched as described above. After extensive rapid washing to remove excessive biotin, cells were returned to growth media supplemented with 10% FBS and cultured at 37 °C in 5% CO_2, 95% air for various time points with fresh media added every 12 h to maintain cell viability. At the indicated time points, cells lysates and biotinylated proteins were obtained as described above and subjected to SDS-PAGE and immunoblotting.

The relative band intensities of the proteins for each time point on the Western blots were obtained through multiple exposures of the same blot to ensure the signal was within the linear range of the x-ray film. Densitometry measurements were obtained using ImageJ™ image processing software.

RESULTS

Role of N-Myristoylation and Ca^{2+} Binding in the Interaction between NHE1 and CHP3—To characterize the biological significance of *N*-myristoylation and Ca^{2+} binding of CHP3 in relation to its regulation of NHE1, the critical glycine residue of the *N*-myristoylation motif at position 2 and the crucial aspartic acid in the EF-hand Ca^{2+}-binding motif at position 123 were mutated separately to alanine (G2A and D123A, respectively) (amino acid sequences shown in supplemental Fig. S1). Although the CHP proteins contain four potential EF-hand domains, only the third domain in CHP3 that contains Asp-123 was shown previously to bind Ca^{2+} (16).

In a prior study (25), we demonstrated that NHE1 interacts with CHP3 when coexpressed in intact cells. To assess whether this interaction is dependent on *N*-myristoylation or Ca^{2+} binding of CHP3, each of the CHP3 constructs (wild-type

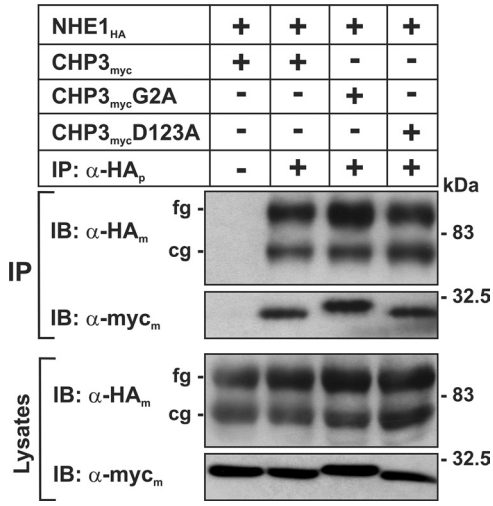

FIGURE 1. ***N*-Myristoylation and Ca^{2+} binding-defective mutants of CHP3 form a complex with NHE1 in transfected cells.** Chinese hamster ovary AP-1 cells stably expressing $NHE1_{HA}$ were transiently transfected with either wild-type or mutant constructs of $CHP3_{myc}$ that are defective in either *N*-myristoylation (G2A) or calcium-binding (D123A). Twenty four hours post-transfection, cell lysates were prepared, and $NHE1_{HA}$-containing protein complexes were immunoprecipitated with a rabbit polyclonal antibody specific to the HA epitope (α-HA_p). The cell lysates and immunoprecipitates (*IP*) were fractionated by SDS-PAGE and analyzed by immunoblotting (*IB*) using mouse monoclonal antibodies specific to either the HA or Myc epitopes (α-HA_m or α-Myc_m, respectively). The two immunoreactive bands visualized in the $NHE1_{HA}$ blots represent the immature core-glycosylated (*cg*) and mature fully glycosylated (*fg*) forms of the exchanger. Data shown are representative of three separate experiments.

(WT), G2A, or D123A) tagged at their C terminus with a Myc epitope ($CHP3_{myc}$) was transiently transfected in the Chinese hamster ovary AP-1 cell line that is devoid of endogenous NHE1 but stably expresses an HA epitope-tagged form of NHE1 ($NHE1_{HA}$). At 24 h post-transfection, cell lysates were obtained and incubated with either a mouse polyclonal antibody that recognizes the HA epitope of $NHE1_{HA}$ or an IgG antibody to control for nonspecific binding. The immunoprecipitated complexes as well as aliquots from the initial cell lysates were subjected to SDS-PAGE and immunoblot analysis to visualize the $NHE1_{HA}$ and $CHP3_{myc}$ proteins. As shown in Fig. 1, all three forms of $CHP3_{myc}$ formed specific complexes with $NHE1_{HA}$. The interaction between $NHE1_{HA}$ and the $CHP3_{myc}$ proteins was verified by the reciprocal experiments of immunoprecipitating $CHP3_{myc}$ and immunoblotting for $NHE1_{HA}$ (data not shown).

To further establish the physical association between $NHE1_{HA}$ and the various CHP_{myc} constructs, their respective subcellular distributions were compared using dual immunolabeling and fluorescence confocal microscopy. Previous studies (25) showed that when coexpressed in AP-1 cells, NHE1 and CHP3 colocalize at the cell surface. However, when CHP3 is expressed in AP-1 cells devoid of NHE1 or coexpressed with mutant forms of NHE1 that do not interact with CHP3, CHP3 fails to accumulate at the cell surface but instead is diffusely distributed throughout the cytoplasm (25). As shown in Fig. 2*A*, WT as well as *N*-myristoylation (G2A) and Ca^{2+} binding (D123A)-defective mutants of $CHP3_{myc}$ colocalized with $NHE1_{HA}$ at the plasma membrane, although there was an increased tendency for the D123A mutant to also accumulate

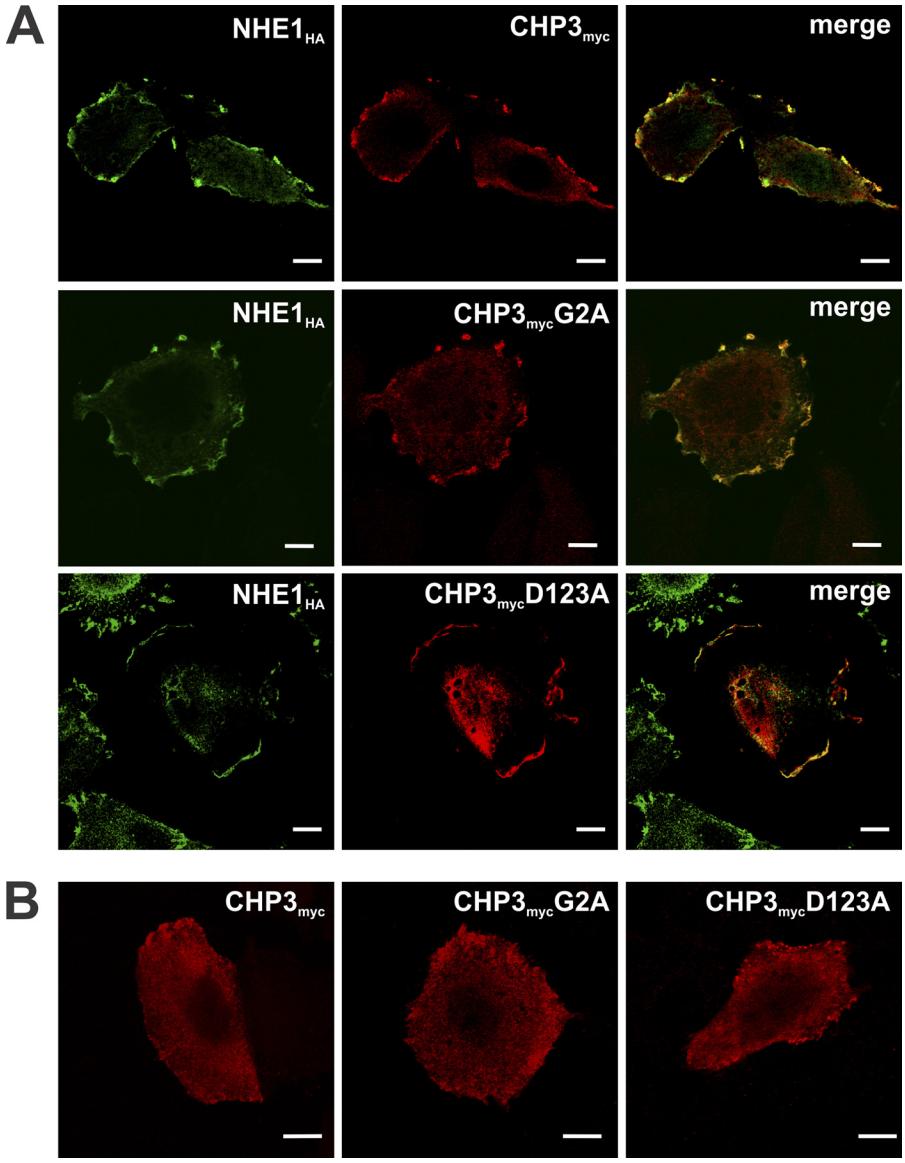

FIGURE 2. ***N*-Myristoylation (G2A) and Ca^{2+} binding (D123A)-defective mutants of CHP3 colocalize with $NHE1_{HA}$ at the plasma membrane.** Immunofluorescence confocal microscopy of AP-1 cells stably expressing $NHE1_{HA}$ and transiently transfected with either wild-type or mutant forms (G2A, D123A) of $CHP3_{myc}$ (*A*) or AP-1 cells transiently transfected with the $CHP3_{myc}$ constructs in the absence of NHE1 (*B*). Subcellular distribution of $NHE1_{HA}$ was visualized using mouse monoclonal antibodies specific to the HA epitope followed by labeling with a goat anti-mouse secondary antibody conjugated to AlexaFluor™-488. $CHP3_{myc}$ distribution was identified through a primary rabbit polyclonal antibody specific to the Myc epitope followed by a secondary goat anti-rabbit antibody conjugated to AlexaFluor™-568. Overlapping signals in the merged images are shown in *yellow*. Data are representative of between two and four independent experiments. *Scale bars* at the *bottom right* of each panel represent 10 μm.

intracellularly (Fig. 2*A*). Consistent with this visual assessment, quantitative statistical analyses of the colocalization of the respective fluorophores indicated strong associations between $NHE1_{HA}$ and $CHP3_{myc}$-WT or -G2A (Pearson's correlation coefficient (r) = 0.87 and 0.68, respectively) and medium correlation between $NHE1_{HA}$ and $CHP3_{myc}$-D123A (r = 0.36). However, in the absence of NHE1, all three forms of CHP3 were distributed more diffusely throughout the cell (Fig. 2*B*). These results demonstrate that *N*-myristoylation and Ca^{2+} binding of CHP3 are not essential for the interaction with NHE1.

Previous studies by Pang *et al.* (17) suggested that Ca^{2+} binding to the two functional EF-hand domains of CHP1 greatly influenced its interaction with NHE1. Furthermore, Gutierrez-Ford *et al.* (16) suggested that CHP3 likely binds Mg^{2+} in its resting state. However, upon cellular stimulation that increases intracellular Ca^{2+}, the Mg^{2+} would be displaced by Ca^{2+}, which then induces a conformational change in CHP3 to an "active" state. To investigate whether the binding of Ca^{2+} to CHP3 influences its interaction with NHE1, we performed a coimmunoprecipitation assay in the absence or presence of 0.1 mM Ca^{2+}. AP-1 cells were transiently cotransfected with $NHE1_{HA}$ and either the WT or mutant D123A construct of $CHP3_{myc}$. After 48 h, cells lysates were prepared in RIPA buffer supplemented with both 1 mM $MgCl_2$ and 1 mM EDTA or with 0.1 mM $CaCl_2$. Cell lysates were incubated with a rabbit polyclonal anti-Myc antibody, and the resulting $CHP3_{myc}$-containing immunoprecipitates were subject to SDS-PAGE and immunoblotting to visualize the extent of association with $NHE1_{HA}$.

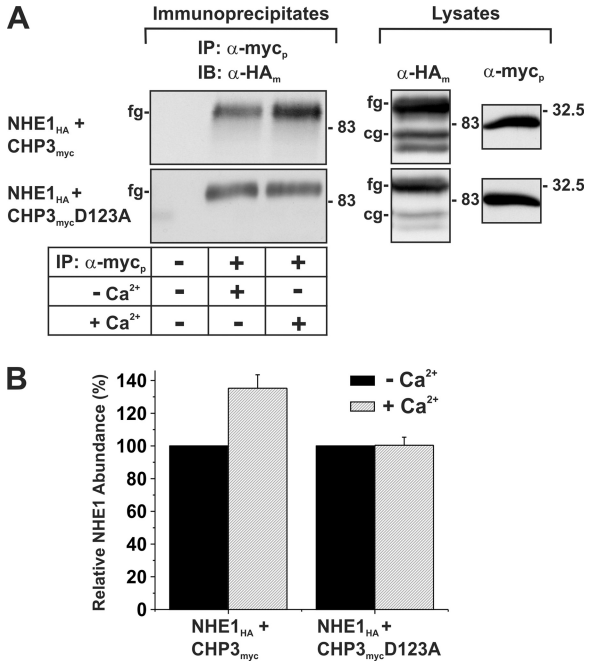

FIGURE 3. **Interaction between NHE1 and CHP3 is influenced by Ca^{2+}.** AP-1 cells were transiently transfected with $NHE1_{HA}$ and either the wild-type or the Ca^{2+} binding-defective mutant of $CHP3_{myc}$. *A*, cell lysates were prepared 48 h post-transfection in RIPA buffer adjusted to contain either 0.1 mM $CaCl_2$ (+*Ca*$^{2+}$) or 1 mM $MgCl_2$ and 1 mM EDTA (−*Ca*$^{2+}$). An aliquot of each cell lysate was removed, and the remaining fractions were subject to immunoprecipitation (*IP*) with a rabbit polyclonal antibody specific to the Myc epitope (α-*myc*$_p$) in their respective RIPA buffer. The protein samples were fractionated by SDS-PAGE and immunoblotting (*IB*). $NHE1_{HA}$ was visualized with a mouse monoclonal antibody specific to the HA epitope (α-*HA*$_m$). *cg*, core-glycosylated; *fg*, fully glycosylated. *B*, intensities of the immunoreactive signals for NHE1 presented in *A* were measured by densitometry using ImageJ® and normalized to the signals obtained in the absence of Ca^{2+} (mean ± S.E., $n = 3$).

As shown in Fig. 3, the amount of $NHE1_{HA}$ that forms a complex with the $CHP3_{myc}$ in the presence of Ca^{2+} was ~35 ± 8% higher compared with conditions containing nominal levels of Ca^{2+}. In the case of the Ca^{2+} binding-deficient $CHP3_{myc}$D123A, there was no detectable difference in its association with NHE1 in the absence or presence of Ca^{2+}. This result indicates that Ca^{2+} is not essential for the binding of CHP3 to NHE1 but does promote a stronger interaction.

N-Myristoylation and Ca^{2+} Binding of CHP3 Are Required for Optimal NHE1 Activity—Previously, we showed that expression of CHP3 increases NHE1 activity by enhancing its biosynthetic maturation and its stability at the plasma membrane, resulting in higher steady-state levels of NHE1 at the cell surface (25). To determine whether *N*-myristoylation or Ca^{2+} binding of CHP3 influences the production and function of NHE1, AP-1 cells that stably express $NHE1_{HA}$ were transiently transfected with an increasing ratio of an expression vector containing either the WT or mutant forms (G2A and D123A) of $CHP3_{myc}$ relative to empty vector. At 24 h post-transfection, the cells were split into two pools, one to obtain corresponding cell lysates to assess its biosynthetic maturation by Western blotting and the other for assessment of NHE1 activity, and then cultured for an additional 24-h period prior to analysis. In agreement with our prior observations (25), increasing expression of WT $CHP3_{myc}$ correlated with enhanced accumulation of both immature core-glycosylated and mature fully glycosylated forms of $NHE1_{HA}$ (Fig. 4*A*), particularly the latter. Because we previously demonstrated that the bulk of fully glycosylated NHE1 resides at the plasma membrane, whereas the core-glycosylated species resides intracellularly (25, 34), we measured the protein levels of fully glycosylated $NHE1_{HA}$ by densitometry and correlated it with NHE1 activity as a function of $CHP3_{myc}$ expression. As shown in Fig. 4, *B* and *C*, WT $CHP3_{myc}$-mediated increases in the abundance of fully glycosylated NHE1 closely paralleled, albeit it to a higher extent, the increases in NHE1 activity (*i.e.* ~2.2-fold *versus* ~1.6-fold, respectively). The reason for the lack of tighter correlation between NHE1 protein abundance and activity is unclear, but it may reflect differences in the sensitivities of the respective methodologies. Alternatively, it could be that not all of the fully glycosylated NHE1 molecules, as measured by densitometry, have yet to reach the cell surface. Similarly, both the *N*-myristoylated and Ca^{2+} binding-defective mutants of $CHP3_{myc}$, which were produced at levels equivalent to WT $CHP3_{myc}$, also increased the abundance and activity of $NHE1_{HA}$, but to lesser extents than WT $CHP3_{myc}$. This suggests that these structural elements, although not critical for the ability of CHP3 to bind and promote the maturation and activity of NHE1, do contribute to its potency.

N-Myristoylation and Ca^{2+} Binding of CHP3 Do Not Influence the Rate of Maturation of Newly Synthesized NHE1—Previously, we showed that CHP3 stimulates the post-translational maturation, cell surface accumulation, and stability of NHE1 (25). The new results presented in Fig. 4 suggested that *N*-myristoylation and Ca^{2+} binding of CHP3 are involved in optimizing cell surface NHE1 abundance and activity. To further investigate the mechanistic basis for this observation, we first investigated the oligosaccharide maturation of NHE1 by using a transient transfection approach to monitor newly synthesized exogenous proteins. Thus, AP-1 cells were transiently transfected with $NHE1_{HA}$ and either empty vector or different constructs of $CHP3_{myc}$ (WT, G2A, or D123A), and the cell lysates were prepared at time points up to 72 h following transfection to assess the expression profiles of $NHE1_{HA}$ and $CHP3_{myc}$. As shown in Fig. 5, $NHE1_{HA}$ alone showed a transitory increase in both core and fully glycosylated forms that reached maximal levels at ~24 h, with the bulk being primarily core-glycosylated. By comparison, although $NHE1_{HA}$ cotransfected with WT $CHP3_{myc}$ also showed a similar temporal increase in expression of both the core and fully glycosylated $NHE1_{HA}$, there was a much greater accumulation of the fully glycosylated relative to the core-glycosylated form, consistent with previous findings (25). Notably, loss of *N*-myristoylation or Ca^{2+} binding of $CHP3_{myc}$ did not impair the rate of processing of newly synthesized $NHE1_{HA}$.

To directly verify that CHP3-mediated increases in fully glycosylated NHE1 protein and transport activity indeed reflect its accumulation at the cell surface, as implied by the data presented in Fig. 4, plasmalemmal NHE1 levels were directly measured using a cell surface biotinylation assay (35). To this end, AP-1 cells were transiently cotransfected with a fixed amount of $NHE1_{HA}$ and an increasing ratio of $CHP3_{myc}$ to empty vector (pCMV). The cells were also cotransfected with an expression

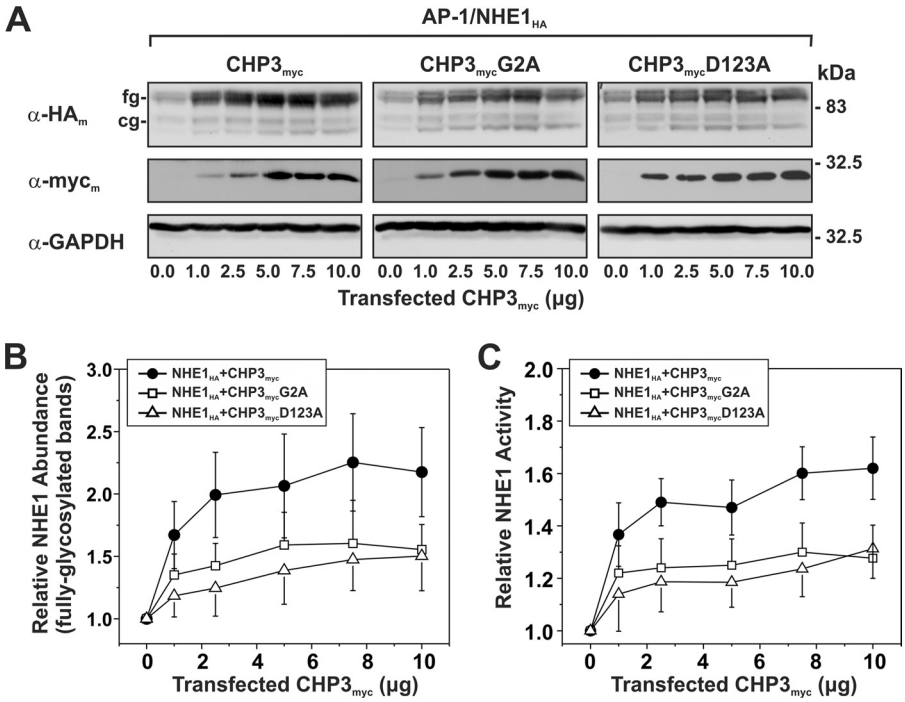

FIGURE 4. ***N*-Myristoylation and Ca^{2+} binding of CHP3 influence NHE1 abundance and activity.** AP-1 cells stably expressing $NHE1_{HA}$ were cultured in a series of 10-cm dishes and transiently transfected with an increasing ratio of wild-type or mutant (G2A or D123A) $CHP3_{myc}$-containing expression plasmids to empty vector (0–10 μg per dish) to maintain the total amount of DNA transfected at 10 μg per dish. At 24 h post-transfection, each plate was split into six wells of a 24-well plate and one well of a 6-well plate to assess $NHE1_{HA}$ activity and protein expression, respectively. *A*, at 48 h post-transfection, cell lysates were prepared and analyzed for $NHE1_{HA}$ and $CHP3_{myc}$ expression by SDS-PAGE and immunoblotting. Immunoreactive bands corresponding to the fully glycosylated (*fg*) and core-glycosylated (*cg*) forms of $NHE1_{HA}$ and CHP_{myc} were detected using a primary mouse monoclonal anti-HA (α-HA_m) and anti-Myc (α-myc_m) antibody, respectively, and a secondary goat anti-mouse antibody conjugated to horseradish peroxidase. As a control for protein loading, the blots were stripped and reprobed for expression of endogenous GAPDH using a primary mouse monoclonal anti-GAPDH antibody (α-*GAPDH*) and a secondary goat anti-mouse antibody conjugated to horseradish peroxidase. *B*, abundance of the fully glycosylated form of $NHE1_{HA}$ in the absence or presence of $CHP3_{myc}$, as presented in *A*, were quantified by densitometric measurements of the immunoreactive signals on x-ray films exposed within the linear range and then analyzed using ImageJ software. The intensity values were normalized to those obtained in the absence of $CHP3_{myc}$. *C*, Na^+/H^+ exchange activity of cells expressing $NHE1_{HA}$ and wild-type or mutant $CHP3_{myc}$ (G2A and D123A) were measured as a function of CHP3 abundance. NHE1 activity was determined as the initial rates of amiloride-inhibitable $^{22}Na^+$ influx (pmol/min/mg total cellular protein) following an acute intracellular acid load induced by prepulsing with NH_4^+, as described under "Experimental Procedures." To facilitate comparison, the activity data were normalized to AP-1/$NHE1_{HA}$ cells that do not express CHP3 ($\sim 8 \pm 2$ pmol/min/mg protein) and represented as relative changes in NHE1 activity. Values represent the mean $\pm$ S.E. of three experiments, each performed in triplicate.

plasmid that constitutively expresses green fluorescent protein (pGFP) as a control for transfection efficiency. Forty eight hours post-transfection, plasma membrane proteins were selectively extracted for analysis of NHE1 abundance by immunoblotting. As illustrated in Fig. 6, the fully glycosylated form of $NHE1_{HA}$ was the predominant species detected at the cell surface, and its increased abundance correlated with enhanced expression of wild-type as well as mutated forms of $CHP3_{myc}$. Hence, *N*-myristoylation and Ca^{2+} binding of CHP3 are not essential elements for CHP3-mediated trafficking of NHE1 to the cell surface, consistent with the microscopy results presented in Fig. 2.

N-Myristoylation and Ca^{2+} Binding of CHP3 Do Not Influence the pH_i Sensitivity of NHE1—Previous studies have indicated that Ca^{2+} binding to the CHP1 isoform was an important determinant of the pH_i sensitivity of NHE1 (17). To examine whether this might also apply to CHP3, the H^+ sensitivity of $NHE1_{HA}$ was measured in the absence or presence of WT and mutant forms of $CHP3_{myc}$. To facilitate measurements of NHE1 pH_i sensitivity, AP-1 cell lines were generated that stably express $NHE1_{HA}$ alone or in combination with the WT, G2A, or D123A variants of $CHP3_{myc}$. In each case, the total abundance of $NHE1_{HA}$ in cells expressing the $CHP3_{myc}$ variants was enhanced compared with cells expressing NHE1 alone (Fig. 7*A*), consistent with the transient transfection assays. The pH_i profile of NHE1 in the various stable cell lines was then assessed by measuring the initial rates of amiloride-inhibitable $^{22}Na^+$ influx at various intracellular H^+ concentrations clamped at values between pH_i 5.4 and 7.4 using the K^+-nigericin method, as described under "Experimental Procedures." The flux rates were normalized to 100% of the exchanger's maximal activity at pH_i 5.4. As shown in Fig. 7*B*, WT and well as *N*-myristoylation- or Ca^{2+} binding-defective $CHP3_{myc}$ did not affect the H^+ affinity of the exchanger.

N-Myristoylation and Ca^{2+} Binding of CHP3 Are Required for Cell Surface Stability of NHE1—Although *N*-myristoylation and Ca^{2+} binding of $CHP3_{myc}$ do not seem to be required for the CHP3-mediated enhancement of post-translational processing of NHE1, the cell surface accumulation and transport activities of the exchanger in AP-1 cells expressing *N*-myristoylation- or Ca^{2+} binding-defective mutants of $CHP3_{myc}$ were nevertheless approximately half that obtained with wild-type $CHP3_{myc}$ (see Fig. 4). This suggests the involvement of another mechanism by which *N*-myristoylation and Ca^{2+} binding of $CHP3_{myc}$ might exert its influence on the exchanger. Apart from promoting the maturation of $NHE1_{HA}$ to the cell surface,

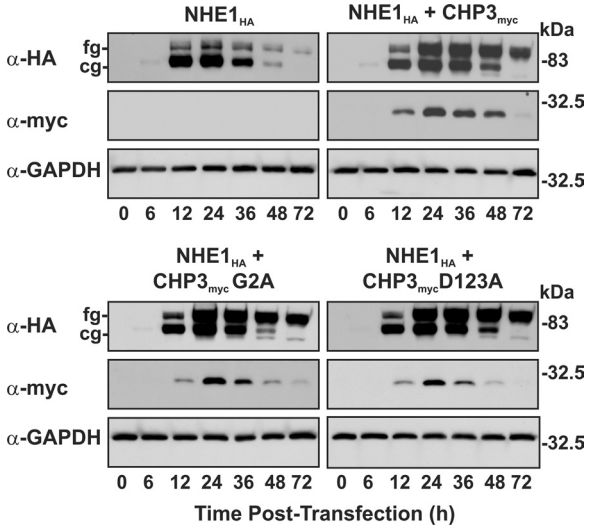

FIGURE 5. **CHP3-mediated oligosaccharide maturation of NHE1 does not require *N*-myristoylation or Ca^{2+} binding.** AP-1 cells were transiently cotransfected with equal quantities of $NHE1_{HA}$ and empty vector or variants of $CHP3_{myc}$ (WT, G2A, and D123A). Cell lysates were prepared at the indicated time points following transfection (0–72 h) and subjected to SDS-PAGE and immunoblotting to detect expression of $NHE1_{HA}$ and $CHP3_{myc}$ as described in the legend to Fig. 4. Blots were stripped and reprobed for expression of endogenous GAPDH as a control for protein loading. Data shown are representative of three independent experiments. *cg*, core-glycosylated; *fg*, fully glycosylated.

$CHP3_{myc}$ is also known to stabilize $NHE1_{HA}$ at the plasma membrane. To test the importance of *N*-myristoylation and Ca^{2+} binding of $CHP3_{myc}$ in this process, the half-life of fully glycosylated $NHE1_{HA}$ alone or together with each of the $CHP3_{myc}$ variants (WT, G2A, and D123A) was measured using a biotinylation pulse-chase assay as described previously (25). Briefly, plasmalemmal proteins of AP-1 cell lines stably expressing $NHE1_{HA}$ alone or in combination with the WT, G2A, or D123A variants of $CHP3_{myc}$ were covalently linked to biotin using the membrane-impermeant reagent sulfo-NHS-SS-biotin. Following removal of excess reagent, the cells were incubated in regular culture media over a 48-h period. At several time points during this period, the biotinylated proteins were extracted from the cell lysates using NeutrAvidin™-Sepharose beads, fractionated by SDS-PAGE, and analyzed by immunoblotting. Expression of cell surface fully glycosylated $NHE1_{HA}$ for the various time points was measured by densitometry, normalized to maximum $NHE1_{HA}$ expression at 0 h, and then plotted as a function of time. As shown in Fig. 8, *A* and *B*, the half-life of biotinylated, fully glycosylated $NHE1_{HA}$ was ~3.8-fold higher in the presence of WT $CHP3_{myc}$ than in its absence (14.5 ± 3.6 h *versus* 3.8 ± 0.6 h, respectively). However, the half-life of $NHE1_{HA}$ in cells coexpressing either the *N*-myristoylation-defective (G2A) or the Ca^{2+} binding-defective (D123A) mutant of CHP3 was considerably reduced (6.1 ± 1.1 and 4.8 ± 0.8 h, respectively) compared with WT $CHP3_{myc}$ and, although intermediate, more closely paralleled that of cells expressing $NHE1_{HA}$ alone (3.8 ± 0.6 h). As a side note, we observed that the total cellular levels of $NHE1_{HA}$ and $CHP3_{myc}$ (WT, G2A, D123A) increased as a function of time in culture. Although the reason for this is unclear, this may relate to the constitutive overproduction of these exogenous proteins when driven transcriptionally by a strong "unregulated" viral promoter (CMV), ultimately resulting in a net increase in their accumulation as a function of cell density and time in culture. However, as the relative increases in NHE1 and CHP3 were similar under each condition, the measurements of NHE1 half-life (*i.e.* derived from NHE1 molecules labeled with biotin at time 0 h) should be comparable.

Overall, the above results indicate that although *N*-myristoylation and Ca^{2+} binding of CHP3 are neither critical for the interaction of CHP3 with NHE1 nor for the early stage maturation of the exchanger, they seem crucial for stabilizing NHE1 at the cell surface and up-regulating its activity.

N-Myristoylation and Ca^{2+} Binding of CHP3 Function Together in Promoting the Cell Surface Activity and Stability of NHE1—Interestingly, the interaction of NHE1 with the *N*-myristoylation- and Ca^{2+} binding-defective mutants of CHP3 appear to elicit the same response. This suggests that the structural integrity of both domains might be jointly required for optimal function of CHP3. Indeed, proteins containing *N*-myristoylation and EF-hand Ca^{2+}-binding domains sometimes function as Ca^{2+}-myristoyl switch proteins, whereby the binding of calcium ions induces a conformational change that extrudes the buried myristoyl group. This, in turn, enables the molecule to bind to the lipid bilayer (30, 36, 37). Indeed, Gutierrez-Ford *et al.* (16) demonstrated that upon binding Ca^{2+}, CHP3 undergoes a change in its secondary structure, albeit small in comparison with other EF-hand proteins. In the absence of a more detailed tertiary structure, it is plausible that this change may be sufficient to expose the myristoylation group that might otherwise be masked within the protein.

To further test the interdependence of these two domains, a double mutation of the $CHP3_{myc}$ protein was produced ($CHP3_{myc}$G2A/D123A) and then assayed for its interaction with and effects on $NHE1_{HA}$ function in transfected AP-1 cells. As shown in supplemental Fig. S2, $NHE1_{HA}$ and $CHP3_{myc}$G2A/D123A readily formed a protein complex, as determined by reciprocal coimmunoprecipitation assays. The abundance and activity of $NHE1_{HA}$ stably expressed in AP-1 cells also increased as a function of increasing expression of transiently transfected $CHP3_{myc}$G2A/D123A (supplemental Fig. S3, *A–C*), findings similar to that observed for the individual mutants of CHP3 (G2A and D123A; as described in Fig. 4) but considerably less than WT $CHP3_{myc}$. Furthermore, this increase in activity occurred without any noticeable difference in the intracellular H^+ affinity of NHE1 (supplemental Fig. S3*D*).

Finally, the cell surface maturation and stability of $NHE1_{HA}$ in the presence of $CHP3_{myc}$G2A/D123A was verified by repeating the cell surface biotinylation and pulse-chase assays. As shown in Fig. 9, the total as well as cell surface levels of $NHE1_{HA}$ increased as a function of the abundance of $CHP3_{myc}$G2A/D123A when transiently expressed in AP-1 cells, results similar to the individual mutations. Likewise, the cell surface half-life (Fig. 10) of the double $CHP3_{myc}$ G2A/D123A mutant (5.0 ± 0.6 h) was markedly reduced compared with WT (14.5 ± 3.6 h) but was not significantly different from the single G2A and D123A mutants (6.1 ± 1.1 and 4.8 ± 0.8 h, respectively; see Fig. 8). These results support the notion that the *N*-myristoylation site and single EF-hand Ca^{2+}-binding domain may operate jointly as a Ca^{2+}-myristoyl switch protein.

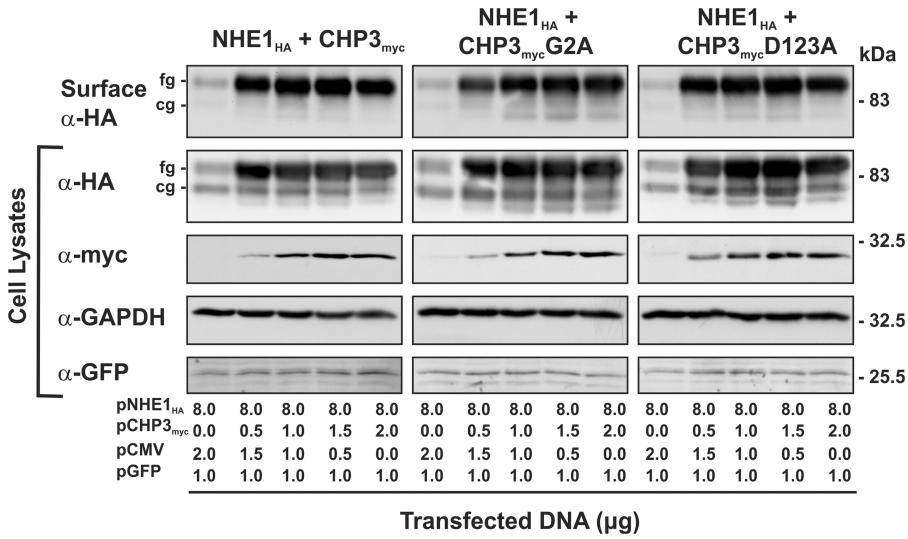

FIGURE 6. **CHP3-mediated trafficking of NHE1 to the cell surface is not dependent on *N*-myristoylation or Ca^{2+} binding of CHP3.** AP-1 cells were grown to subconfluence on 10-cm dishes and then transiently transfected with a fixed amount of expression plasmid DNA containing $NHE1_{HA}$ (8 μg) and an increasing ratio of $CHP3_{myc}$ (WT, G2A, or D123A) to empty expression vector (*pCMV*) (0–2 μg per dish). Cells were also simultaneously cotransfected with a plasmid that expresses green fluorescent protein (*pGFP*) as a control for transfection efficiency. At 48 h post-transfection, cells were subjected to surface biotinylation as described under "Experimental Procedures," and whole cell lysates were prepared. A major fraction of the lysates was subsequently incubated with NeutrAvidin-Sepharose beads to isolate the biotinylated cell surface proteins. Aliquots of the whole cell lysates and biotinylated cell surface proteins were subjected to SDS-PAGE and immunoblotting. Expression of fully glycosylated (*fg*) and core-glycosylated (*cg*) forms of $NHE1_{HA}$ and $CHP3_{myc}$ were detected as described in Fig. 4. GFP was detected using a primary rabbit polyclonal anti-GFP antibody (*α-GFP*) and a secondary goat anti-rabbit antibody conjugated to horseradish peroxidase. Immunoblots of the lysates were stripped and reprobed for endogenous GAPDH as a control for protein loading. Data shown are representative of three independent experiments.

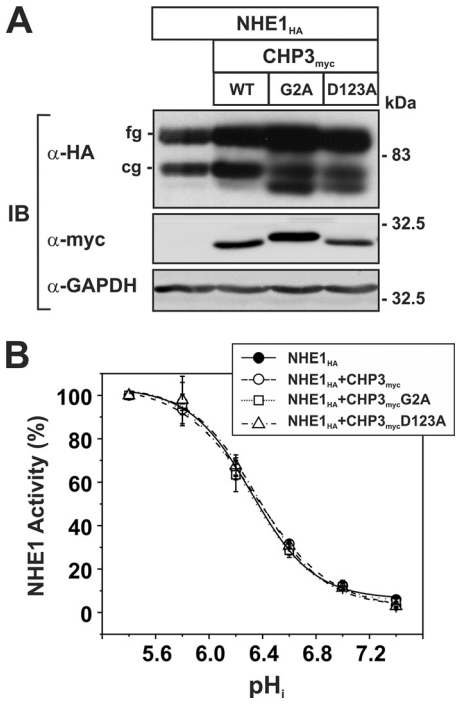

FIGURE 7. **Affinity of NHE1 for intracellular H^+ is unaffected by CHP3.** AP-1 cell lines were generated that stably express $NHE1_{HA}$ alone or stably coexpress $NHE1_{HA}$ and each of the $CHP3_{myc}$ constructs (WT, G2A, or D123A). *A*, expression of $NHE1_{HA}$ and the $CHP3_{myc}$ constructs was assessed by SDS-PAGE and immunoblotting (*IB*). *cg*, core-glycosylated; *fg*, fully glycosylated. *B*, initial rates of amiloride-inhibitable $^{22}Na^+$ influx were measured at various intracellular H^+ concentrations over the range of pH_i 5.4–7.4. The pH_i value was adjusted by the K^+-nigericin method, as described under "Experimental Procedures." To facilitate comparison of the effects of CHP3, the data were normalized to their respective maximal rates of uptake. Values represent the mean ± S.E. of three experiments, each performed in triplicate. *Error bars* smaller than the symbol are absent.

DISCUSSION

CHP3 is the most recently identified member of a family of *N*-myristoylated, EF-hand Ca^{2+}-binding proteins that bind to the cytoplasmic juxtamembrane C termini of plasma membrane-type NHEs and regulate their activities in unique, albeit overlapping, ways (18, 20, 25, 26, 38). Previously, we reported that CHP3 promotes the oligosaccharide maturation and trafficking of NHE1 along the exocytic pathway as well as its half-life and transport activity at the cell surface (25). To better understand the molecular mechanisms underlying this regulation, we examined the potential relevance of the *N*-myristoylation site and single Ca^{2+}-binding domain of CHP3 to this process using a site-directed mutagenesis approach.

Here, we show that *N*-myristoylation or Ca^{2+} binding are neither essential for the interaction of CHP3 with NHE1 nor are they necessary for CHP3-mediated oligosaccharide maturation and trafficking of the transporter to the plasma membrane. However, disruption of either structural element markedly diminished the ability of CHP3 to enhance the steady-state abundance and corresponding activity of NHE1 at the plasma membrane to a similar extent, effects that were not further altered by a double mutation. This change correlated with a significant reduction in the cell surface stability of the exchanger.

The observation that the *N*-myristoylation and Ca^{2+} binding-defective mutants of CHP3 were able to enhance the post-translational maturation and surface delivery of NHE1 at rates comparable with WT CHP3 suggests that other structural domains of CHP3 are engaged in this process upon binding NHE1. Although the precise mechanism is unknown, this could conceivably involve CHP3-dependent recruitment of components implicated in protein trafficking. Such a suggestion is not

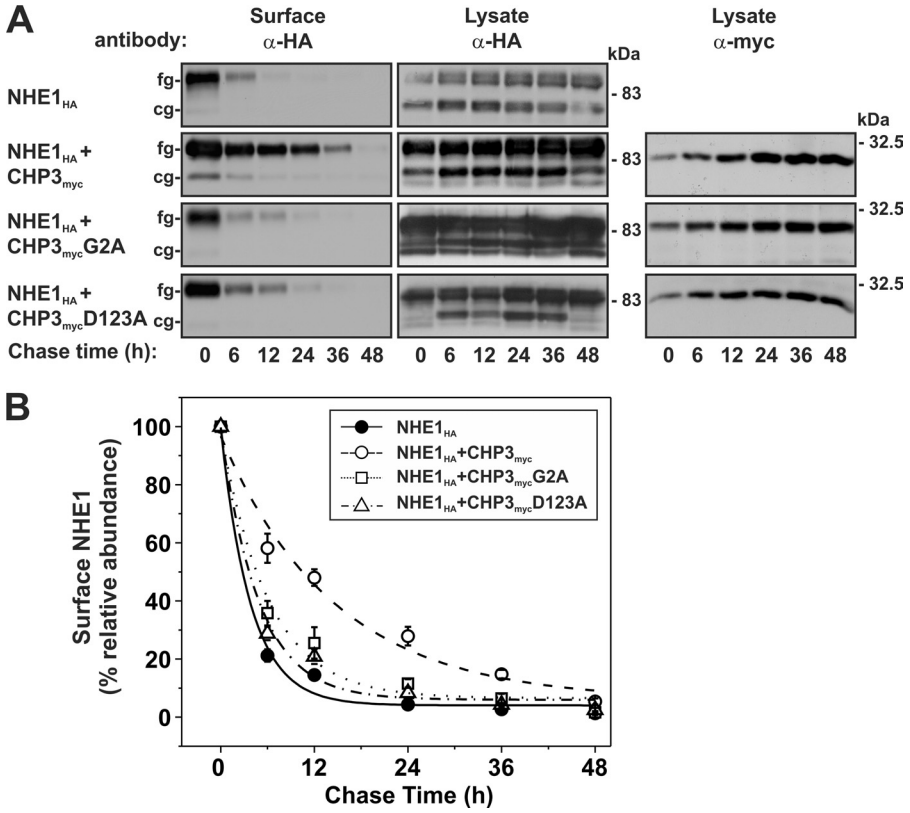

FIGURE 8. ***N*-Myristoylation and Ca^{2+} binding of CHP3 enhance cell surface stability of NHE1.** *A*, AP-1 cells stably expressing $NHE1_{HA}$ or stably coexpressing $NHE1_{HA}$ and individual variants of $CHP3_{myc}$ (WT, G2A, and D123A) were subject to cell surface biotinylation, as described under "Experimental Procedures." The cells were returned to growth media at 37 °C, and then cell lysates were prepared at varying times over a 48-h period. At each time point, a small fraction of the cell lysates was removed for immunoblotting, and the remainder was incubated with NeutrAvidin-Sepharose beads to extract the biotinylated proteins. Total cellular levels of core-glycosylated (*cg*) and fully (*fg*) glycosylated $NHE1_{HA}$ and $CHP3_{myc}$ as well as levels of surface-biotinylated, fully glycosylated $NHE1_{HA}$ were monitored as a function of time by SDS-PAGE and immunoblotting, as described in the legend to Fig. 4. It was noted that occasionally a small amount of the core-glycosylated $NHE1_{HA}$ was detected in the cell surface biotinylated fraction, possibly indicating contamination from intracellular compartments. However, when the blots were stripped and reprobed for intracellular GAPDH, no signal was detected (data not shown). This suggests that a minor fraction of the core-glycosylated NHE1 can traffic to the plasma membrane, perhaps as a consequence of overexpression. *B,* data represent densitometric analysis of the cell surface fully glycosylated $NHE1_{HA}$ presented in *A*, normalized as a percentage of its maximal abundance at time 0 h and plotted as a function of time. Values represent the mean ± S.E. of three experiments. *Error bars* smaller than the symbol are absent.

without precedent, as previous studies (39) have shown that its paralog CHP1/p22 interacts with the multifunctional protein GAPDH that facilitates the binding of CHP1/p22 to microtubules independent of its association with microsomal membranes (and associated cargo). Whether GAPDH also fulfills a similar role for CHP3 remains to be determined. Notwithstanding, it would appear that *N*-myristoylation and Ca^{2+} binding of CHP3 are not required for the early events in NHE1 processing but are required at the plasma membrane to increase the residency time of the transporter.

At present, there is little tertiary structure information available for CHP3. However, the finding that the individual as well as double mutations yielded identical behavior suggests that these distant sites are mechanically and functionally linked in a manner that would be consistent with a Ca^{2+}-myristoyl switch mechanism, as has been described for some *N*-myristoylated Ca^{2+}-binding proteins such as recoverin and guanylate cyclase-activating proteins (36, 40, 41). In this regard, we observed that although a functional Ca^{2+}-binding site was not required for the assembly of an NHE1·CHP3 complex at nominal Ca^{2+} concentrations, elevation of Ca^{2+} levels to micromolar levels significantly increased the *in vitro* binding strength of wild-type CHP3 to NHE1, effects that were abrogated by mutating the Ca^{2+}-binding site. Previous analyses by Gutierrez-Ford *et al.* (16) showed that recombinant CHP3 binds a single Ca^{2+} ion in the third predicted EF-hand domain with an apparent affinity (K_d) of ~0.8 μM, a value that is within the physiological range for sensing changes in intracellular Ca^{2+}. Furthermore, by measuring intrinsic tryptophan fluorescence, they detected a small but significant Ca^{2+}-dependent conformational change in CHP3. Although the precise meaning of this structural perturbation remains to be determined, it could conceivably enhance the affinity of CHP3 for NHE1 while at the same time exposing the *N*-myristoylation site, thereby facilitating the attachment of CHP3 to the inner leaflet of the membrane. In principle, this might strengthen the retention of the NHE1·CHP3 complex at the cell surface. Furthermore, such an arrangement could also act to align the juxtamembrane cytoplasmic C terminus of NHE1 in close proximity to the inner membrane surface that may be important for transport activity. Indeed, previous studies (34) have shown that the CHP-binding site of NHE1 is situated between two positively charged amino acid clusters that form an electrostatic interaction with phosphatidylinositol 4,5-bisphosphate embedded in the inner leaflet of the plasma membrane, which could further strengthen the orientation of that segment of the C terminus of NHE1 in tight

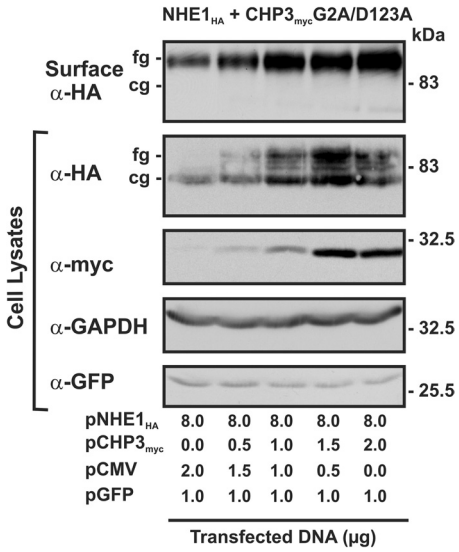

FIGURE 9. **Loss of both *N*-myristoylation and Ca^{2+} binding of CHP3 does not impair oligosaccharide maturation and cell surface delivery of NHE1.** AP-1 cells (10-cm dishes) were cotransfected with a fixed amount of $NHE1_{HA}$ (8 μg/plate) and an increasing ratio of $CHP3_{myc}$G2A/D123A expression vector (0–2 μg/plate) to empty vector as described in Fig. 7. As a control for transfection efficiency, 1 μg of an expression vector containing GFP (pGFP) was also transfected. At 24 h post-transfection, cell surface proteins were biotinylated for 30 min on ice, and after removal of excess biotin, cell lysates were obtained. A small fraction of protein was removed for immunoblotting, and the remaining lysates were incubated with NeutrAvidin™-agarose beads to extract cell surface $NHE1_{HA}$. All proteins were then subjected to SDS-PAGE and immunoblotting with monoclonal antibodies that recognize the HA and Myc epitopes to visualize $NHE1_{HA}$ and $CHP3_{myc}$, respectively. As a control for equal loading and transfection efficiency, blots were stripped and reprobed with a monoclonal antibody specific to endogenous GAPDH and GFP. *fg*, fully glycosylated; *cg*, core-glycosylated.

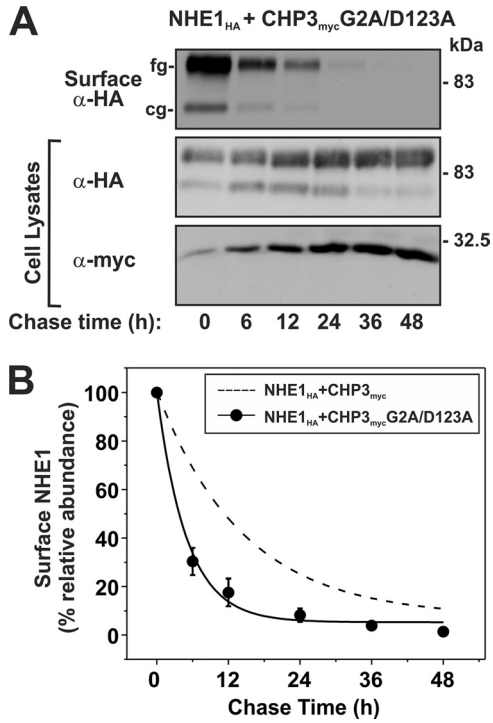

FIGURE 10. **Loss of both *N*-myristoylation and Ca^{2+} binding of CHP3 decreases cell surface stability of NHE1.** AP-1 cells stably expressing $NHE1_{HA}$ and the combined *N*-myristoylation- and Ca^{2+} binding-defective CHP3 mutant (G2A/D123A) were seeded equally in a 6-well plate and cultured to subconfluence. *A*, surface proteins were biotinylated for 30 min on ice, and after removal of excess biotin, cells were returned to regular growth media supplemented with 10% FBS and antibiotics and incubated at 37 °C, 5% CO_2 in humidified atmosphere. At the indicated time points, cell lysates were obtained and, after removal of a small fraction for Western blotting, were subject to incubation overnight at 4 °C with NeutrAvidin™-agarose beads to extract surface-labeled $NHE1_{HA}$. Proteins were separated by SDS-PAGE and immunoblotted to visualize the remaining surface $NHE1_{HA}$ as a function of time as described in the legend to Fig. 8. *B*, intensities of the immunoreactive signals for surface $NHE1_{HA}$ were measured by densitometry using ImageJ™ software, normalized to maximum expression at time 0 h, and plotted as a function of time. For comparative purposes, the plot was overlaid with the data describing the effect of wild-type CHP3 on NHE1 cell surface stability shown in Fig. 8.

juxtaposition to the membrane. Experimental manipulations that disrupted this association significantly decreased NHE1 activity. Hence, such a configuration may enhance the stability and optimal transport of the transporter. Thus, CHP3 appears to act as a positive effector of NHE1 cell surface stability and activity under basal conditions, but it also has the potential to further enhance NHE1 function under conditions that increase intracellular Ca^{2+} within the physiological range. Thus, besides ubiquitous Ca^{2+}/calmodulin that is known to stimulate NHE1 (42, 43), the additional presence of CHP3 in tissues such as heart and brain might be particularly beneficial as they are subject to more dynamic fluctuations in intracellular Ca^{2+} and pH.

The functional relevance of *N*-myristoylation and Ca^{2+} binding has also been examined in the context of the NHE1·CHP1 complex. Similar to CHP3, mutation of the *N*-myristoylation site in CHP1 did not alter the binding, membrane trafficking, or pH_i sensitivity of NHE1 (17). However, the contributions of Ca^{2+} binding to CHP1 function appear to differ markedly from those of CHP3. Unlike CHP3, CHP1 contains two very high affinity Ca^{2+}-binding domains (EF3 and EF4), which increase their avidity for Ca^{2+} by ~45-fold (K_d ~90 → 2 nM) upon the formation of a complex with the CHP-binding domain of NHE1 (17, 44). Given that resting intracellular Ca^{2+} concentrations are estimated to be ~100 nM, CHP1 would bind Ca^{2+} constitutively. Single mutations that prevent Ca^{2+} binding to either EF3 or EF4, while not impairing its binding to NHE1, caused a significant reduction in its pH_i sensitivity (17). This shift to more acidic values reduced basal NHE1 activity and markedly impaired its activation by various extracellular stimuli. Moreover, disruption of both Ca^{2+}-binding sites abolished the interaction of CHP1 with NHE1, resulting in the accumulation of the Ca^{2+} binding-defective CHP1 in the cytoplasm. Thus, Pang *et al.* (17) concluded that the two Ca^{2+}-binding domains of CHP1 most likely do not act collectively as a Ca^{2+} sensor but rather as important structural elements that help to control the pH_i sensing of NHE1. This behavior is in contrast to that of the Ca^{2+} binding-defective CHP3, which retains its ability to bind to NHE1 without altering its pH_i sensitivity. Although the molecular basis for this isoform difference is unclear, CHP3 possesses three other helix-loop-helix structural domains in addition to its one functional EF-hand Ca^{2+}-binding domain that are more divergent in sequence compared with CHP1 and CHP2, and therefore they might be uniquely arranged to better stabilize the protein through intramolecular EF-hand pairing (45). In the case of CHP1 (and possibly CHP2), the mutations that prevent Ca^{2+} binding may impart a more severe structural deformation that prevents further interactions with its remain-

ing helix-loop-helix structures needed to interact with NHE1. Thus, with respect to the NHE1·CHP1 complex, the role of the *N*-myristoylation remains unclear, but it does not appear to be functionally coupled to the Ca^{2+}-binding domains.

In summary, this study provides further insight into the roles of *N*-myristoylation and Ca^{2+} binding of CHP3 and its regulation of NHE1. CHP3 regulates the processing and stability of cell surface NHE1, and although *N*-myristoylation and Ca^{2+} binding are not required for binding and for maturation of the exchanger, they play a crucial role in stabilizing NHE1 at the plasma membrane to promote optimal Na^+/H^+ exchange activity.

Acknowledgment—We kindly thank Kimberley Young for assistance with the quantitative statistical analyses of the colocalization image data presented in this paper.

REFERENCES

1. Casey, J. R., Grinstein, S., and Orlowski, J. (2010) Sensors and regulators of intracellular pH. *Nat. Rev. Mol. Cell Biol.* **11,** 50–61
2. Kapus, A., Grinstein, S., Wasan, S., Kandasamy, R., and Orlowski, J. (1994) Functional characterization of three isoforms of the Na^+/H^+ exchanger stably expressed in Chinese hamster ovary cells. ATP dependence, osmotic sensitivity, and role in cell proliferation. *J. Biol. Chem.* **269,** 23544–23552
3. Denker, S. P., Huang, D. C., Orlowski, J., Furthmayr, H., and Barber, D. L. (2000) Direct binding of the Na-H exchanger NHE1 to ERM proteins regulates the cortical cytoskeleton and cell shape independently of H^+ translocation. *Mol. Cell* **6,** 1425–1436
4. Tominaga, T., and Barber, D. L. (1998) Na-H exchange acts downstream of RhoA to regulate integrin-induced cell adhesion and spreading. *Mol. Biol. Cell* **9,** 2287–2303
5. Denker, S. P., and Barber, D. L. (2002) Cell migration requires both ion translocation and cytoskeletal anchoring by the Na-H exchanger NHE1. *J. Cell Biol.* **159,** 1087–1096
6. Putney, L. K., and Barber, D. L. (2003) Na-H exchange-dependent increase in intracellular pH times G_2/M entry and transition. *J. Biol. Chem.* **278,** 44645–44649
7. Dyck, J. R., and Fliegel, L. (1995) Specific activation of the Na^+/H^+ exchanger gene during neuronal differentiation of embryonal carcinoma cells. *J. Biol. Chem.* **270,** 10420–10427
8. Li, X., Karki, P., Lei, L., Wang, H., and Fliegel, L. (2009) Na^+/H^+ exchanger isoform 1 facilitates cardiomyocyte embryonic stem cell differentiation. *Am. J. Physiol. Heart Circ. Physiol.* **296,** H159–H170
9. Wu, K. L., Khan, S., Lakhe-Reddy, S., Wang, L., Jarad, G., Miller, R. T., Konieczkowski, M., Brown, A. M., Sedor, J. R., and Schelling, J. R. (2003) Renal tubular epithelial cell apoptosis is associated with caspase cleavage of the NHE1 Na^+/H^+ exchanger. *Am. J. Physiol. Renal Physiol.* **284,** F829–F839
10. Schelling, J. R., and Abu Jawdeh, B. G. (2008) Regulation of cell survival by Na^+/H^+ exchanger-1. *Am. J. Physiol. Renal Physiol.* **295,** F625-F632
11. Orlowski, J., and Grinstein, S. (2004) Diversity of the mammalian sodium/proton exchanger SLC9 gene family. *Pflugers Arch.* **447,** 549–565
12. Orlowski, J., and Grinstein, S. (2011) Na^+/H^+ exchangers. *Compr. Physiol.* **1,** 2083–2100
13. Meima, M. E., Mackley, J. R., and Barber, D. L. (2007) Beyond ion translocation. Structural functions of the sodium-hydrogen exchanger isoform-1. *Curr. Opin. Nephrol. Hypertens* **16,** 365–372
14. Di Sole, F., Vadnagara, K., Moe, O. W., and Babich, V. (2012) Calcineurin homologous protein. A multifunctional Ca^{2+}-binding protein family. *Am. J. Physiol. Renal Physiol.* **303,** F165–F179
15. Lin, X., Sikkink, R. A., Rusnak, F., and Barber, D. L. (1999) Inhibition of calcineurin phosphatase activity by a calcineurin B homologous protein. *J. Biol. Chem.* **274,** 36125–36131
16. Gutierrez-Ford, C., Levay, K., Gomes, A. V., Perera, E. M., Som, T., Kim, Y. M., Benovic, J. L., Berkovitz, G. D., and Slepak, V. Z. (2003) Characterization of tescalcin, a novel EF-hand protein with a single Ca^{2+}-binding site. Metal-binding properties, localization in tissues and cells, and effect on calcineurin. *Biochemistry* **42,** 14553–14565
17. Pang, T., Hisamitsu, T., Mori, H., Shigekawa, M., and Wakabayashi, S. (2004) Role of calcineurin B homologous protein in pH regulation by the Na^+/H^+ exchanger 1. Tightly bound Ca^{2+} ions as important structural elements. *Biochemistry* **43,** 3628–3636
18. Pang, T., Su, X., Wakabayashi, S., and Shigekawa, M. (2001) Calcineurin homologous protein as an essential cofactor for Na^+/H^+ exchangers. *J. Biol. Chem.* **276,** 17367–17372
19. Inoue, H., Nakamura, Y., Nagita, M., Takai, T., Masuda, M., Nakamura, N., and Kanazawa, H. (2003) Calcineurin homologous protein isoform 2 (CHP2), Na^+/H^+ exchanger-binding protein, is expressed in intestinal epithelium. *Biol. Pharm. Bull.* **26,** 148–155
20. Pang, T., Wakabayashi, S., and Shigekawa, M. (2002) Expression of calcineurin B homologous protein 2 protects serum deprivation-induced cell death by serum-independent activation of Na^+/H^+ exchanger. *J. Biol. Chem.* **277,** 43771–43777
21. Jin, Q., Kong, B., Yang, X., Cui, B., Wei, Y., and Yang, Q. (2007) Overexpression of CHP2 enhances tumor cell growth, invasion and metastasis in ovarian cancer. *In Vivo* **21,** 593–598
22. Li, G. D., Zhang, X., Li, R., Wang, Y. D., Wang, Y. L., Han, K. J., Qian, X. P., Yang, C. G., Liu, P., Wei, Q., Chen, W. F., Zhang, J., and Zhang, Y. (2008) CHP2 activates the calcineurin/nuclear factor of activated T cells signaling pathway and enhances the oncogenic potential of HEK293 cells. *J. Biol. Chem.* **283,** 32660–32668
23. Perera, E. M., Martin, H., Seeherunvong, T., Kos, L., Hughes, I. A., Hawkins, J. R., and Berkovitz, G. D. (2001) Tescalcin, a novel gene encoding a putative EF-hand Ca^{2+}-binding protein, Col9a3, and renin are expressed in the mouse testis during the early stages of gonadal differentiation. *Endocrinology* **142,** 455–463
24. Levay, K., and Slepak, V. Z. (2007) Tescalcin is an essential factor in megakaryocytic differentiation associated with Ets family gene expression. *J. Clin. Invest.* **117,** 2672–2683
25. Zaun, H. C., Shrier, A., and Orlowski, J. (2008) Calcineurin B homologous protein 3 promotes the biosynthetic maturation, cell surface stability, and optimal transport of the Na^+/H^+ exchanger NHE1 isoform. *J. Biol. Chem.* **283,** 12456–12467
26. Matsushita, M., Tanaka, H., Mitsui, K., and Kanazawa, H. (2011) Dual functional significance of calcineurin homologous protein 1 binding to Na^+/H^+ exchanger isoform 1. *Am. J. Physiol. Cell Physiol.* **301,** C280–C288
27. Maurer-Stroh, S., Eisenhaber, B., and Eisenhaber, F. (2002) N-terminal *N*-myristoylation of proteins. Prediction of substrate proteins from amino acid sequence. *J. Mol. Biol.* **317,** 541–557
28. O'Callaghan, D. W., and Burgoyne, R. D. (2003) Role of myristoylation in the intracellular targeting of neuronal calcium sensor (NCS) proteins. *Biochem. Soc. Trans.* **31,** 963–965
29. Strynadka, N. C., and James, M. N. (1989) Crystal structures of the helix-loop-helix calcium-binding proteins. *Annu. Rev. Biochem.* **58,** 951–998
30. Ames, J. B., Ishima, R., Tanaka, T., Gordon, J. I., Stryer, L., and Ikura, M. (1997) Molecular mechanics of calcium-myristoyl switches. *Nature* **389,** 198–202
31. Rotin, D., and Grinstein, S. (1989) Impaired cell volume regulation in Na^+-H^+ exchange-deficient mutants. *Am. J. Physiol.* **257,** C1158–C1165
32. Orlowski, J. (1993) Heterologous expression and functional properties of amiloride high affinity (NHE-1) and low affinity (NHE-3) isoforms of the rat Na/H exchanger. *J. Biol. Chem.* **268,** 16369–16377
33. Bolte, S., and Cordelières, F. P. (2006) A guided tour into subcellular colocalization analysis in light microscopy. *J. Microsc.* **224,** 213–232
34. Aharonovitz, O., Zaun, H. C., Balla, T., York, J. D., Orlowski, J., and Grinstein, S. (2000) Intracellular pH regulation by Na^+/H^+ exchange requires phosphatidylinositol 4,5-bisphosphate. *J. Cell Biol.* **150,** 213–224
35. Le Bivic, A., Real, F. X., and Rodriguez-Boulan, E. (1989) Vectorial targeting of apical and basolateral plasma membrane proteins in a human adenocarcinoma epithelial cell line. *Proc. Natl. Acad. Sci. U.S.A.* **86,** 9313–9317

36. Zozulya, S., and Stryer, L. (1992) Calcium-myristoyl protein switch. *Proc. Natl. Acad. Sci. U.S.A.* **89,** 11569–11573
37. Ladant, D. (1995) Calcium and membrane binding properties of bovine neurocalcin delta expressed in *Escherichia coli*. *J. Biol. Chem.* **270,** 3179–3185
38. Mailänder, J., Müller-Esterl, W., and Dedio, J. (2001) Human homolog of mouse tescalcin associates with Na^+/H^+ exchanger type-1. *FEBS Lett.* **507,** 331–335
39. Andrade, J., Pearce, S. T., Zhao, H., and Barroso, M. (2004) Interactions among p22, glyceraldehyde-3-phosphate dehydrogenase, and microtubules. *Biochem. J.* **384,** 327–336
40. Ames, J. B., and Ikura, M. (2002) Structure and membrane-targeting mechanism of retinal Ca^{2+}-binding proteins, recoverin, and GCAP-2. *Adv. Exp. Med. Biol.* **514,** 333–348
41. Ames, J. B., Lim, S., and Ikura, M. (2012) Molecular structure and target recognition of neuronal calcium sensor proteins. *Front. Mol. Neurosci.* **5,** 10
42. Bertrand, B., Wakabayashi, S., Ikeda, T., Pouysségur, J., and Shigekawa, M. (1994) The Na^+/H^+ exchanger isoform 1 (NHE1) is a novel member of the calmodulin-binding proteins. Identification and characterization of calmodulin-binding sites. *J. Biol. Chem.* **269,** 13703–13709
43. Wakabayashi, S., Bertrand, B., Ikeda, T., Pouysségur, J., and Shigekawa, M. (1994) Mutation of calmodulin-binding site renders the Na^+/H^+ exchanger (NHE1) highly H^+-sensitive and Ca^{2+} regulation-defective. *J. Biol. Chem.* **269,** 13710–13715
44. Mishima, M., Wakabayashi, S., and Kojima, C. (2007) Solution structure of the cytoplasmic region of Na^+/H^+ exchanger 1 complexed with essential cofactor calcineurin B homologous protein 1. *J. Biol. Chem.* **282,** 2741–2751
45. Niki, I., Yokokura, H., Sudo, T., Kato, M., and Hidaka, H. (1996) Ca^{2+} signaling and intracellular Ca^{2+}-binding proteins. *J. Biochem.* **120,** 685–698